Cooperative luminescence in Yb^{3+}-doped phosphate glasses

2003 J. Phys.: Condens. Matter 15 4877

(http://iopscience.iop.org/0953-8984/15/27/319)

INSTITUTE OF PHYSICS PUBLISHING JOURNAL OF PHYSICS: CONDENSED MATTER

J. Phys.: Condens. Matter **15** (2003) 4877–4887 PII: S0953-8984(03)60522-9

Cooperative luminescence in Yb^{3+}-doped phosphate glasses

M J V Bell[1], W G Quirino[1], S L Oliveira[2], D F de Sousa[2,3] and L A O Nunes[2]

[1] Departamento de Física, Universidade Federal de Juiz de Fora, 36036-330, Juiz de Fora, MG, Brazil
[2] Instituto de Física de São Carlos, Universidade de São Paulo, Caixa Postal 369, São Carlos, SP, 13560-970, Brazil
[3] Institut für Laser-Physik, Universität Hamburg, Jungiusstraße 9a, 20355 Hamburg, Germany

E-mail: mjbell@fisica.ufjf.br

Received 6 March 2003, in final form 14 May 2003
Published 27 June 2003
Online at stacks.iop.org/JPhysCM/15/4877

Abstract

In this paper we present results on cooperative luminescence performed on Yb^{3+}-doped metaphosphate glasses under 980 nm excitation. We have measured emission spectra and decay lifetimes in the visible and infrared regions as a function of Yb concentration. It was observed that, up to 10% of Yb concentration, cooperative emission increases while lifetime is observed to decrease. Such behaviour is attributed to the Yb interaction with OH^- radicals and energy migration among Yb ions.

1. Introduction

Cooperative luminescence is an up-conversion process in which two interacting ions (dimers) in the excited state decay simultaneously to the ground state, emitting one photon at twice the energy of single-ion transitions [1, 2]. This process relies on Coulomb interaction between ions and has a strong dependence on inter-ionic distances. Among rare earths, Yb^{3+} is the most investigated because it presents only one electronic excited state at around 1000 nm in the $4f^n$ configuration [3]. In this case, there is a simultaneous de-excitation of two excited Yb^{3+} ions in the $^2F_{5/2}$ level, resulting in the emission of one visible photon at around 500 nm. The large energy gap between Yb^{3+} ground and metastable multiplets also reduces unfavorable non-radiative de-excitation processes such as multi-phonon relaxation and quenching due to OH^- groups compared to other rare-earth ions. Even though up-conversion processes that involve a resonant intermediate energy level, for example energy transfer or excited state absorption, are about 10^5 times more efficient than cooperative luminescence, the latter has been observed in several highly doped Yb systems [4–15].

Table 1. The concentration (N) and thickness (d) of the samples used in the present work.

	0.2Yb	0.5Yb	1.5Yb	3Yb	5Yb	6Yb	10Yb	15Yb
N ($\times 10^{20}$ cm^{-3})	0.23	0.56	1.53	3.02	4.79	5.96	9.72	13.4
d (cm)	0.302	0.402	0.380	0.380	0.335	0.382	0.226	0.384

There have been many articles published about cooperative emission in Yb-doped glasses and crystals. Nevertheless, the influence of processes such as radiation trapping (due to the superposition of the absorption and emission Yb^{3+} bands) and energy transfer (migration among Yb ions or interaction with impurities) has not been discussed in detail. To obtain Yb-doped systems for optical devices, the evaluation of such processes is required. Among the possible applications reported for cooperative emission in Yb-doped systems, the most important are three-dimensional planar displays [10], intrinsic bistability for optical switching [4, 13, 16], and planar lasers for optical devices in telecommunications [14].

In this paper we have measured emission spectra and lifetimes in the visible and near-infrared regions as a function of Yb concentration. The influence of radiation trapping and the energy transfer to OH^- groups on the cooperative emission is presented and discussed.

2. Experimental set-up

The glasses used in the present work have the following composition: $(60 - x)(NaPO_3)_3$–$40Al(PO_3)_3$–xYb_2O_3 with $x = 0.2$, 0.5, 1.5, 3, 5, 6, 10 and 13 wt% (hereafter called xYb). The glasses were prepared using reagent-grade $(NaPO_3)_3$ and $Al(PO_3)_3$ using the conventional melt quenching method. The powders were mixed in the desired proportions and melted in porcelain crucibles at temperatures between 750 and 1150 °C in air, and poured into a previously heated brass mould. The chemical composition of each glass was measured using an energy-dispersive x-ray spectrometer (LEO 440-EDX Oxford detector). It was verified that the analysed compositions of the glasses are similar to the batched compositions. Table 1 shows the measured Yb concentration (in ions cm^{-3}) and the thicknesses of the samples. Absorption spectra were taken using a Magna FT–IR Nicolet 850 spectrophotometer. Luminescence at 980 nm was achieved by a CW Ar^+ laser tuned at 476 nm. Luminescence was dispersed by a 0.25 m Jarrel–Ash monochromator and analysed using an InGaAs detector connected to a lock-in amplifier. The decay time of the $^5F_{5/2} \rightarrow {}^5F_{7/2}Yb^{3+}$ transition was recorded using a germanium detector connected to a Tektronix oscilloscope. Cooperative luminescence was obtained with laser excitation at 980 nm, dispersed by a SPEX 1403 double spectrograph and collected by a N_2-cooled CCD detector. Appropriate filters were used to suppress scattered laser light. Temporal transients at 500 nm were obtained using a modulated 980 nm diode laser. Modulation was achieved using a mechanical chopper with frequencies in the range of 10–100 Hz, according to the sample lifetime. The signal emitted by the samples passed through infrared filters to avoid the luminescence at 980 nm and was collected by a GaAs photomultiplier connected to a digital oscilloscope. All measurements were made at room temperature.

3. Results

Figure 1(a) presents the absorption spectrum of the 6Yb sample, attributed to the $^2F_{7/2} \rightarrow {}^2F_{5/2}Yb^{3+}$ transition. The inset shows the integrated absorption band as a function of Yb concentration, which exhibits a linear dependence as expected. Figure 1(b) displays the

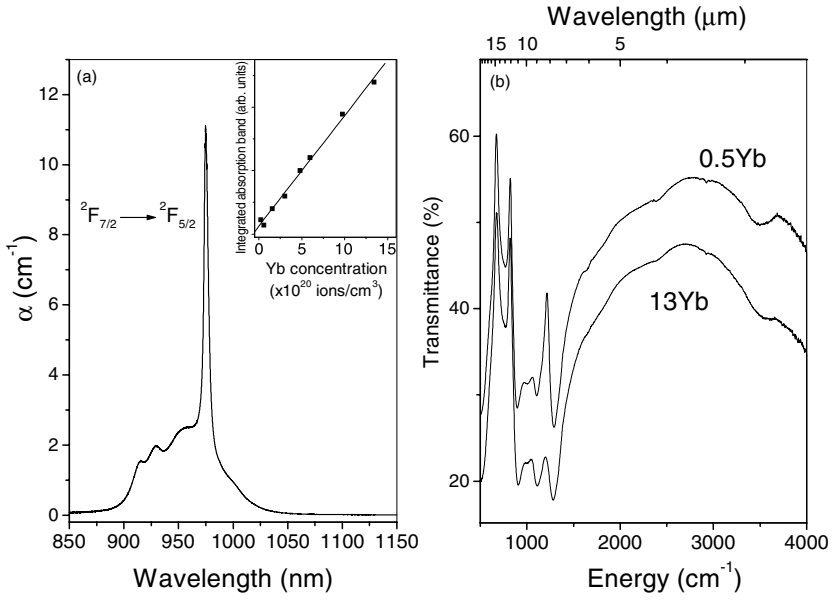

Figure 1. (a) The Yb^{3+} absorption spectrum for the 6Yb sample, at room temperature. The inset shows the integrated band as a function of Yb concentration. (b) The infrared spectra of the 0.5Yb and 13Yb samples, in the range 500–4000 cm^{-1}.

near-infrared transmission in the region of 500–4000 cm^{-1} (20–2.5 μm) for samples 0.5Yb and 13Yb. It is important to mention that these particular measurements were performed in samples with a thickness of 0.57 mm. The region from 500 to 1500 cm^{-1} exhibits metaphosphate glass structures [17]. The absorption bands at 3500 and 2400 cm^{-1} are attributed to the presence of OH^- radicals. In phosphate glasses, OH^- groups can be present at different positions on the phosphate chain, which gives rise to different OH^- associations. This difference results in a number of overlapping absorption bands which, combined, give a broad band that extends from 2700 to 3700 cm^{-1}. Another important point is that the water content is nearly the same for both samples.

Figure 2 displays the near-infrared luminescence as a function of Yb^{3+} concentration, pumped at 476 nm. In this case there is small absorption from the glassy host, followed by energy transfer to the Yb ions. The line-shape of the spectra is due to the inhomogeneous broadening characteristic of glassy hosts. The large bandwidth is attributed to the transitions from Stark sublevels of the $^2F_{5/2}$ and $^2F_{7/2}$ Yb^{3+} levels. Specifically, the transition at 975 nm originates from radiative transition from the lowest Stark sublevel of the $^2F_{5/2}$ level to the lowest Stark sublevel of the $^2F_{7/2}$ level. The inset shows the integrated intensity of the $^2F_{5/2} \rightarrow {}^2F_{7/2}Yb^{3+}$ emission band, which increases almost linearly with Yb concentration.

The cooperative luminescence of the samples is shown in figure 3. The spectra are characterized by a broad band with about 20 nm of HWHM (half width at half maximum), centred at 500 nm. The main peaks at 496 and 502 nm may be attributed to the combination of electronic energies of the Stark levels of isolated Yb^{3+} ions. There is a small red shift in energy, which is attributed to second-order correction of the double excitation energy, as explained by Dexter [18]. It can also be noted that the cooperative luminescence line-shape, called $f_{\mathrm{coop}}(E)$, undergoes a change depending on the Yb concentration. It is known that $f_{\mathrm{coop}}(E)$ is proportional to the self-convolution integral of the near-infrared line-shape, $f_{\mathrm{IR}}(E)$, as follows:

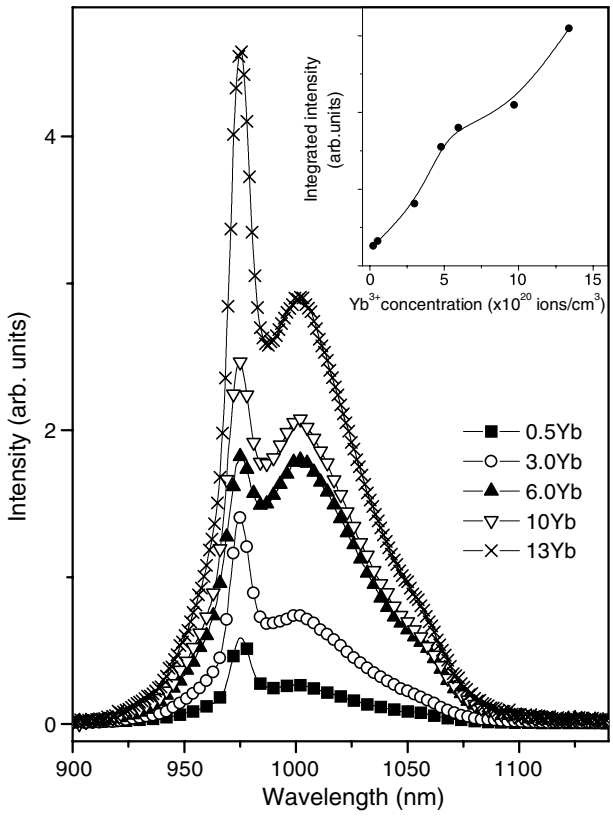

Figure 2. Near-infrared luminescence, attributed to the $^2F_{5/2} \rightarrow {}^2F_{7/2}Yb^{3+}$ transition, as a function of Yb concentration. The laser excitation was tuned at 476 nm. The inset shows the integrated intensity of the luminescence band as a function of Yb concentration.

$f_{\text{coop}}(E) \propto \int f_{(\text{IR})}(E')\, f_{(\text{IR})}(E-E')\, \mathrm{d}E'$ [19]. So, it can be seen that $f_{\text{coop}}(E)$ will be modified according to the changes of the near-infrared line-shapes shown in figure 2. The inset shows the cooperative integrated intensity, which increases up to 10% (9.72×10^{21} ions cm^{-3}) and is followed by quenching for higher Yb concentrations.

Figure 4 depicts the near infrared and cooperative lifetimes as a function of Yb concentration. Two features should be emphasized. One is that the near infrared and cooperative lifetimes decrease with Yb concentration, indicating the presence of nonradiative decay channels. The other is that cooperative lifetimes are about half of their respective near infrared ones. The continuous line resulted from fitting procedures to be discussed in the next section.

4. Discussion

The decrease in lifetime as Yb concentration increases indicates that nonradiative processes should play an important role. Considering that the decay time achieved for the 0.2Yb sample could correspond to the radiative lifetime τ_0, then the nonradiative rate (W_{nr}) may be obtained from $W_{\text{nr}} = 1/\tau - 1/\tau_0$, where τ is the measured lifetime. Figure 5 shows that W_{nr} increases with Yb concentration. The observed features may occur by different mechanisms. The most

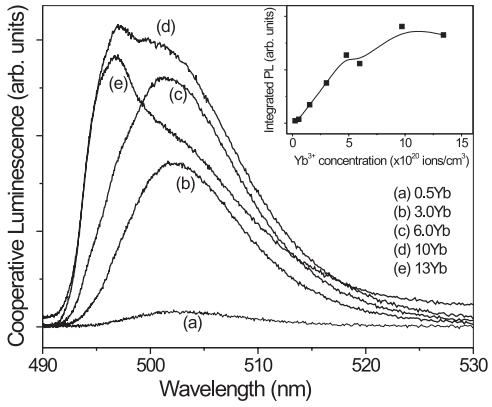

Figure 3. The cooperative luminescence and integrated intensity (inset) as a function of Yb concentration. Samples were excited at 980 nm.

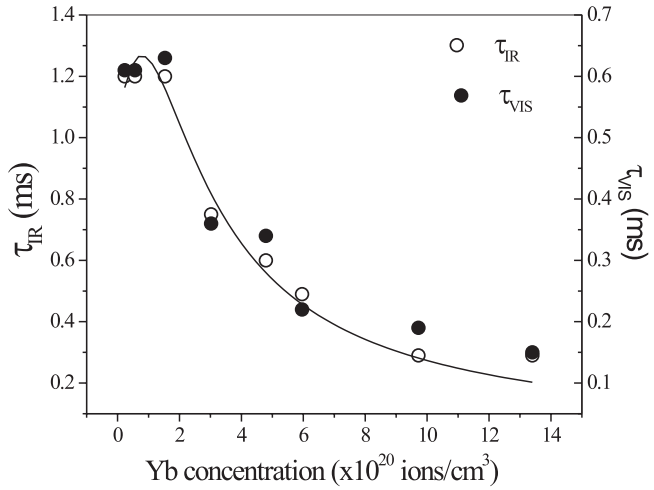

Figure 4. Lifetimes of the near-infrared and cooperative emissions as a function of Yb concentration. The continuous curve corresponds to fitting procedures.

likely are: (1) energy migration among Yb^{3+} ions, followed by transfer to recombination centres; (2) interaction between Yb^{3+} ions and the glassy host defects; (3) trapping by defects such as OH^-; and (4) radiation trapping of energy among Yb ions. The result is an increase in lifetimes, as observed in the samples.

We discuss these effects in detail in the following.

4.1. Nonradiative processes

Among the nonradiative processes mentioned, we propose that energy migration and the presence of OH^- radicals, whose energies occur in the range 2700–3700 cm^{-1}, are the most important. This is based on the following considerations:

(a) Near-infrared spectra of the samples demonstrated the presence of absorption bands in the region mentioned.

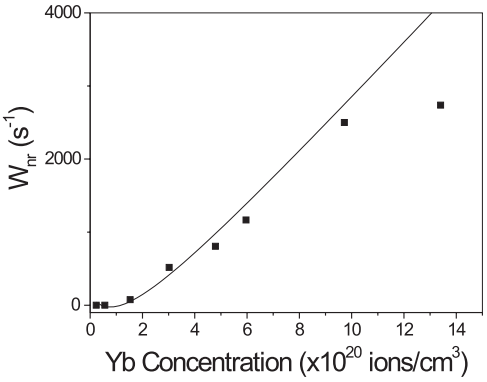

Figure 5. The nonradiative transition rate, W_{nr}, as a function of Yb concentration. The continuous curve represents the fitting by means of the equation $W_{nr} = (1/\tau_0)[1 + \tau_0(140N + 270N^2)]/(1 + 0.5N) - 1/\tau_0$, where N is the Yb^{3+} concentration and τ_0 represents the radiative lifetime.

(b) The OH^- content is nearly the same in all samples.
(c) Preliminary studies conducted on samples prepared in a controlled atmosphere (in vacuum) with the same Yb concentrations demonstrated that the cooperative emission is two orders of magnitude stronger, under the same experimental conditions. Moreover, the infrared spectra evidenced that the OH^- content is significantly reduced in this set of samples.
(d) Energy migration among Yb ions followed by energy transfer to defects depends on the superposition between absorption and emission cross sections, and is proportional to the square of Yb concentration.

It is well known that the superposition mentioned is very strong in Yb ions [20–22]. In [23], dos Santos *et al* considered that energy migration between Yb^{3+} ions, followed by energy transfer to defects, was the most important mechanism in non-hygroscopic tellurite glasses.

In this way, we consider W_{nr} to be composed of two contributions:

$$W_{nr} = W_{OH} + W_{em} \tag{1}$$

where W_{OH} is the nonradiative decay by OH^- radicals and W_{em} is the energy migration nonradiative process. The first needs only three interactions with these radicals, which is more probable than decay by phonons, with energies around 1200 cm^{-1} for the present samples. Zhang and Hu have shown that OH^- impurities are very effective quenchers of the Yb luminescence. The energy transfer rate to OH^- impurities is proportional to the acceptor and donor concentration [24, 25]. The model considers the interaction of OH^- groups and Yb^{3+} ions as follows: the OH^- radicals are coupled to a fraction of Yb ions, which is dependent on the OH^- concentration in the glass. Nonradiative quenching occurs after the excited energy is transferred to the Yb ions coupled to the OH^- groups. The excited energy will be lost whenever it is transferred to a Yb ion coupled to an OH^- quenching centre. In this way, the donors (Yb ions) and acceptors (Yb ions coupled to OH^- groups) may be treated as proposed in [24, 25]:

$$W_{OH} = (k_{OH})(\alpha_{OH})N_{Yb} = c_1 N_{Yb} \tag{2}$$

where k_{OH} is a constant that determines the force of the interactions between Yb ions and OH^- radicals, N_{Yb} is the donor concentration (Yb), α_{OH} corresponds to the OH^- content, and c_1 is the proportionality constant. The term $c_1 N_{Yb}$ will be used in units of 10^{20} ions cm^{-3}. It is clear that W_{OH} increases with Yb concentration due to the decrease of the distance between donors and acceptors. Such behaviour has been verified experimentally in several systems [24, 25].

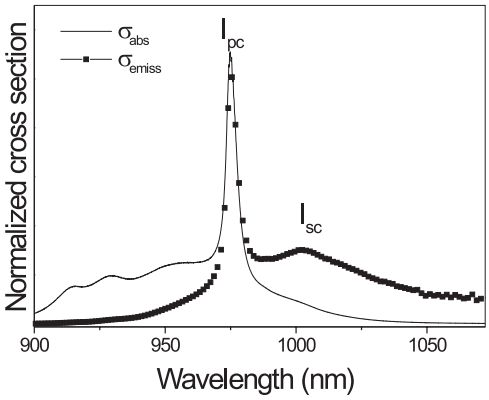

Figure 6. The absorption and emission cross sections for the $^2F_{7/2} \rightarrow {}^2F_{5/2}Yb^{3+}$ transition. The emission cross section was obtained from the reciprocity method.

Turning back to the energy migration W_{em}, in the dipole–dipole approximation it is given by [26]:

$$W_{em} = \frac{3\hbar^4 c^4}{4\pi^4 \tau}\left(\frac{1}{R}\right)^6 Q \int \frac{F_e(E)F_a(E)\,dE}{E^4} = c_2 N_{Yb}^2 \tag{3}$$

where R is the inter-ionic distance, Q is the integrated absorption cross section $\int \sigma(E)\,dE$, $F_e(E)$ ($F_a(E)$) is the normalized shape of emission (absorption) spectra, and c_2 is the proportionality constant. Performing the above calculations, we found $W_{em} = 270N_{Yb}^2$, using N_{Yb} in units of 10^{20} ions cm^{-3}.

So, $W_{nr} = c_1 N_{Yb} + 270N_{Yb}^2$, where c_1 is to be determined by fitting procedures.

4.2. Radiation trapping

Radiation trapping has been observed in several Yb^{3+}-doped systems [27–29]. In this case, spontaneously emitted photons are trapped by re-absorption by Yb ions in the $^2F_{7/2}$ ground state and subsequently emitted again in such a way that the entire process is repeated. The net result is that the $^2F_{5/2}$-level lifetime increases. The effect depends on the superposition of the absorption and emission cross sections, as well as on the sample thickness.

Zhang and Hu [24] proposed that radiation trapping could be evaluated by determining the emission cross section theoretically. We obtained the emission cross section using the reciprocity method [21], as shown in figure 6. Then, the parameter rtc (radiation trapping coefficient), defined as $rtc = (I_{pc}/I_{sc} - I_{pm}/I_{sm})/(I_{pc}/I_{sc})$, could give a quantification of the effect, as displayed in figure 7. Here, I_{pc} (I_{pm}) represents the principal calculated (measured) peak and I_{sc} (I_{sm}) corresponds to the secondary calculated (measured) peak. From the figure, it is clear that radiation trapping depends on Yb concentration and occurs even for doping levels of about 0.2%, which corresponds to 2.3×10^{19} cm^{-3}. Zhang and Hu [24] reported similar results for the rtc parameter in Yb tetraphosphate glasses.

Auzel [29] proposed that the increase in the radiative lifetime (τ_0) from the radiation trapping effect is given by the factor $(1 + \sigma d N_{Yb})$, where d is the thickness of the samples and σ is the absorption cross section. In our case, $\sigma = 1.4 \times 10^{-20}$ cm^2 and d is around 0.35 cm for all the samples (the average value, according to table 1).

So, the lifetime of the near infrared emission should include at least two competing terms: (a) the trapping of radiation, which tends to increase the lifetime; and (b) nonradiative losses

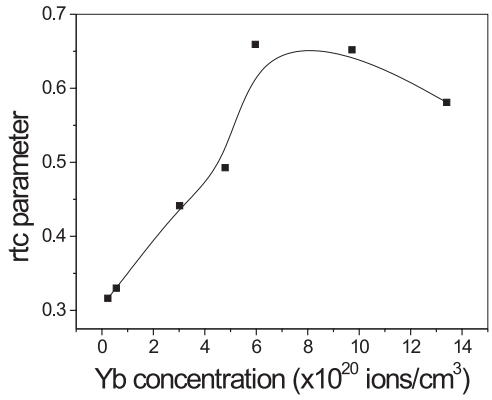

Figure 7. The radiation trapping coefficient (rtc) as a function of Yb concentration.

by OH^- interaction and energy migration among Yb ions:

$$\tau = \tau_0 \frac{(1 + 0.5N_{\mathrm{Yb}})}{[1 + \tau_0(c_1 N_{\mathrm{Yb}} + 270N_{\mathrm{Yb}}^2)]}. \tag{4}$$

The result of the fitting is shown in figure 4 (continuous curve), which exhibits a good agreement with the experimental results. The radiative lifetime obtained is $\tau_0 = 1.05$ ms and the parameter $c_1 = (140 \pm 20)$ cm^3 s^{-1} results in $(k_{\mathrm{OH}})(\alpha_{\mathrm{OH}}) = 1.4 \times 10^{-18}$ cm^3 s^{-1}, which is comparable to that reported by Zhang and Hu [24] given by 4.5×10^{-18} cm^3 s^{-1} for Yb-doped tetraphosphate glasses. Additionally, the continuous line shown in figure 5 was achieved with the same parameters for W_{nr}.

Considering that the cooperative lifetime follows the same behaviour as the near-infrared lifetime, it can be concluded that the presence of OH^- radicals as well as energy migration also affects the cooperative properties.

We propose that the dependence of the cooperative and near-infrared intensities (I_{coop} and I_{ir}, respectively) on Yb concentration can be described theoretically by a rate equation that includes the nonradiative losses W_{nr} [19]:

$$\frac{\mathrm{d}N_2}{\mathrm{d}t} = PN_1 - W_{21}N_2 - XN_2^2 - W_{\mathrm{nr}}N_2 \tag{5}$$

where N_i ($i = 1, 2$) stands for the population of levels 1 and 2, which correspond to the $^2F_{7/2}$ and $^2F_{5/2}$ Yb^{3+} levels, respectively, $N_1 + N_2 = N_{\mathrm{Yb}}$ gives the total concentration of Yb, W_{21} is the radiative rate of the $^2F_{5/2}$ level, and X is the cooperative rate. This depends on the inter-ionic distance, glassy host and multi-polar coupling mechanisms such as electric and magnetic dipole, and so on [30]. Equation (5) means that population of the $^2F_{5/2}$ level is increased by a pumping term PN_1 that depends on the laser intensity (I) according to $P = \sigma I$, where P is the pumping rate and σ is the absorption cross section. All other terms are responsible for losses: $W_{21}N_2$ represents the radiative decay to the $^2F_{7/2}$ level; $W_{\mathrm{nr}}N_2$ accounts for nonradiative losses; and XN_2^2 indicates the loss of population of the $^2F_{5/2}$ level by the creation of Yb pairs.

In this work we have considered $W_{21} = 952$ s^{-1}, and W_{nr} values were extracted from figure 5. From the absorption spectrum at 980 nm, the corresponding pumping rate is $P = 22$ s^{-1}.

The main features of the exposed rate equation are already known [6] and were not changed by the inclusion of the term W_{nr}:

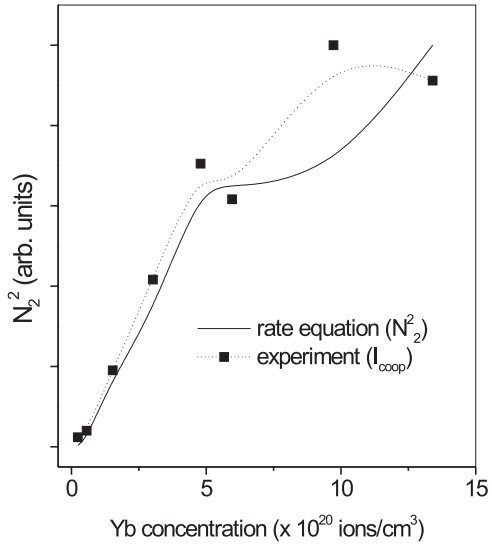

Figure 8. Experimental (I_{coop}) and theoretical (N_2^2) cooperative emission. I_{coop} is proportional to N_2^2.

(1) The X parameter is usually very small due to the fact that the cooperative emission is very weak when compared with the near-infrared emission. So, the system is not sensitive to X and it cannot be determined by fitting procedures. In other words, this means that, even though the term XN_2^2 should be considered as a loss term for N_2 population, it can be neglected when compared to $W_{21}N_2$.

(2) The N_1 population is not significantly changed for the pumping rates of the experiment (up to 22 s^{-1}).

(3) The intensity of the near-infrared emission (I_{ir}) depends on N_2, while cooperative emission (I_{coop}) is proportional to $(N_2)^2$.

(4) I_{ir} and I_{coop} vary linearly and quadratically with P, respectively.

(5) The predicted cooperative lifetime is half of the near-infrared lifetime, given by 0.6 and 1.2 ms, respectively, for the 0.2Yb sample.

The basic change with inclusion of the nonradiative losses is that the model predicts the behaviour of the lifetimes and intensities of the cooperative luminescence as a function of Yb concentration. Figure 8 shows that there is a good comparison between the cooperative luminescence predicted by the above rate equation and the experimental results.

Cooperative luminescence of Yb^{3+} ions has been observed in different crystals and glasses. Some properties are reported in table 2 for purposes of comparison. It should be stressed that the cooperative rates X are obtained experimentally, while the theoretical value—including exchange, electrostatic and magnetic interactions—predicts a value of about 0.02 s^{-1} for Yb interaction distances in the range 3–5 Å [30]. From table 2, it can be noted that the X values are of the same order of magnitude, irrespective of the host. Moreover, all experimental cooperative rates are about one order of magnitude greater than those predicted by theory. This suggests that there are effects, such as higher-order interactions, other than dipole quadrupole coupling as well as the formation of clusters, which need to be considered.

Table 2. Cooperative luminescence parameters reported in other Yb-doped glasses and crystals.

Matrix	Concentration	Interionic distance (Å)	Lifetime (ms)	X (s^{-1})	References
Phosphate	$(0.23–13.4) \times 10^{20}$ ions cm^{-3}	5–20	1.2	—	This work
$CsCdBr_3$	2.3×10^{20} ions cm^{-3}	4–5.5	0.78	0.13	[19]
$Gd_3Ga_5O_{12}$	7×10^{20} ions cm^{-3}	—	1.47	0.37	[8]
$LiNbO_3$	0.5–4 mol%	3.8	0.4		[9]
SiO_2	0.06–1 mol%	—	1.7		[10]
YAG	15 at.%	7.8	0.887	0.29	[14]
La_2O_3	0.5 mol%	—	—	—	[12]
$YbPO_4$	0.5 mol%		0.998		[1]
$MgO–2Li_2O–P_2O_5$	0.2 wt%	5.5	0.938	0.5 to 2	[15]

5. Conclusions

This paper has presented results on the cooperative emission of radiation, which converts near-infrared photons to blue. It has been shown that nonradiative effects play a fundamental role and that the main nonradiative paths were attributed to OH^- radicals (since the samples were obtained in a non-controlled atmosphere) and energy migration among Yb ions. It was observed experimentally that there is an optimum Yb concentration—in this case 10 wt% of Yb. For higher concentrations, nonradiative processes quench the cooperative luminescence. The behaviour of the cooperative luminescence as a function of Yb concentration was described theoretically by the inclusion of the nonradiative losses in the rate equation.

Acknowledgments

This work was partially supported by the Brazilian Agencies Capes, CNPq and FAPESP.

References

[1] Nakazawa E and Shionoya S 1970 *Phys. Rev. Lett.* **25** 1710
[2] Kushida T 1973 *J. Phys. Soc. Japan* **34** 1318
[3] Dieke G H 1968 *Spectra and Energy Levels of Rare Earth Ions in Crystals* (New York: Interscience Publishers)
[4] Lüthi S R, Hehlen M P, Riedener T and Güdel H U 1998 *J. Lumin.* **76/77** 447
[5] Hehlen M P and Güdel H U 1993 *J. Chem. Phys.* **98** 1768
[6] Goldner Ph, Schaudel B, Prassas M and Auzel F 2000 *J. Lumin.* **87–89** 688
[7] Auzel F, Meichenin D, Pelle F and Goldner P 1994 *Opt. Mater.* **4** 35
[8] Courrol L C, Samad R E and Madej C 2000 *Ann. Braz. Comission Opt.* **2** 102
[9] Montoya E, Espeso O and Bausá L E 2000 *J. Lumin.* **87–89** 1036
[10] Maciel G S, Biswas A, Kapoor R and Prasad P N 2000 *Appl. Phys. Lett.* **76** 1978
[11] Auzel F and Goldner P 2001 *Opt. Mater.* **16** 93
[12] Wegh R T and Meijerink A 1995 *Chem. Phys. Lett.* **246** 495
[13] Gamelin D R, Luthi R and Gudel H U 2000 *J. Phys. Chem.* B **104** 11045
[14] Malinowski M, Kaczan M, Piradowckz R, Frukacz Z and Sarnecki J 2001 *J. Lumin.* **94/95** 29
[15] Schaudel B, Goldner P, Prassas M and Auzel F 2000 *J. Alloys Compounds* **300** 443
[16] Hehlen M P, Güdel H U, Shu Q, Rai J, Rai S and Rand S C 1994 *Phys. Rev. Lett.* **73** 1103
[17] Karabulut M, Metwalli E and Brow R K 2001 *J. Non-Cryst. Solids* **283** 211
[18] Dexter D L 1962 *Phys. Rev.* **126** 1962
[19] Goldner Ph, Pelle F, Meichenin D and Auzel F 1997 *J. Lumin.* **71** 137
[20] Kassab L R P, Courrol L C, Morais A S, Mendes C M S P, Tatumi S H, Wetter N U, Gomes L and Salvador V L R 2002 *J. Non-Cryst. Solids* **304** 233
[21] Yin H, Deng P, Zhang J and Gan F 1997 *Mater. Lett.* **30** 29

[22] Jiang C, Liu H, Zeng Q, Tang X and Gan F 2000 *J. Phys. Chem. Solids* **61** 1217
[23] dos Santos P V, Vermelho M V D, Gouveia E A, de Araújo M T, Gouveia-Neto A S, Cassanjes F C, Ribeiro S J L and Messaddeq Y 2002 *J. Chem. Phys.* **116** 6772
[24] Zhang L and Hu H 2001 *J. Non-Cryst. Solids* **292** 108
[25] Zhang L and Hu H 2002 *J. Phys. Chem. Solids* **63** 575
[26] Burshtein Z, Kalisky Y, Levy S Z, Le Boulanger P and Rotman S 2000 *IEEE J. Quantum Electron.* **36** 1000
[27] Laversenne L, Guyot Y, Goutaudier C, Cohen-Adad M Th and Boulon G 2001 *Opt. Mater.* **16** 475
[28] Sumida D S and Fan T Y 1994 *Opt. Lett.* **17** 1343
[29] Auzel F, Bonfigli F, Gagliari S and Baldacchini G 2001 *J. Lumin.* **94/95** 293
[30] Goldner Ph, Pelle F and Auzel F 1997 *J. Lumin.* **72–74** 901